Chemical Engineering Journal 539 (2026) 177307

Contents lists available at ScienceDirect

Chemical Engineering Journal

journal homepage: www.elsevier.com/locate/cej

Stacked quantum dot organic light-emitting diodes in an industrial-grade inkjet printing process

Byoung-Hwa Kwon [a,*], Jin-Wook Shin [a], Chul Woong Joo [a], Chan-mo Kang [a], Hyunsu Cho [a], Sukyung Choi [a], Yoonsung Yoo [a], Hyungwoo Suh [a], Dong-Kyun Shin [b], Jaeryul Yu [b], Yeon Soo Lee [c], Seongju Kim [d], Sungjune Jung [d], Chun Sakong [e], Chun-Won Byun [a], Nam Sung Cho [a]

[a] Reality Display Research Section, Electronics and Telecommunications Research Institute, Daejeon, 34129, Republic of Korea
[b] Gosantech, Cheonan, 31094, Republic of Korea
[c] DUKSAN Neolux, Co., Ltd., Cheonan, 31094, Republic of Korea
[d] Department of Materials Science and Engineering, Pohang University of Science and Technology, 77 Cheongam-Ro, Pohang, 37673, Republic of Korea
[e] ChemE, Daejeon, 34129, Republic of Korea

ARTICLE INFO

Keywords:
Stacked QD-OLED
Inkjet printing
Color conversion
Pixel-defining layer

ABSTRACT

Quantum dot organic light-emitting diode (QD-OLED) displays offer advantages such as wide color gamut, excellent viewing angles, and high contrast ratios. In addition, QD-OLED technology holds significant potential as a core technology for various next-generation displays, including micro-LEDs, OLED on silicon, and reflective displays. This paper reports the development of a novel stacked QD-OLED panel that outperforms QD-OLED panels currently under development in the display industry. Compared with existing QD-OLED displays, the stacked QD-OLED developed in this study can simplify the panel manufacturing process and reduce manufacturing costs by applying a continuous vertical stacking process on a single substrate. Furthermore, the stacked QD-OLED offers structural advantages at the device and panel levels that can suppress optical interference in high-resolution displays. In particular, the fabrication of QD pixels for the stacked QD-OLED is demonstrated using QD ink, a black pixel-defining layer (PDL) photoresist, and inkjet printing components and equipment suited for industrial-scale display manufacturing. A black PDL material with a high aspect ratio and a process technology that operates below 100 °C, essential for realizing stacked QD-OLED panels, are introduced. Finally, by integrating industrially applicable materials, processes, and equipment technologies, a novel stacked QD-OLED panel with a total of 184,800 subpixels and a resolution of 141 pixels per inch, equivalent to that of a 65-inch 8K television, was successfully demonstrated through a 6-inch large-area manufacturing process.

1. Introduction

Quantum dot organic light-emitting diode (QD-OLED) technology is a next-generation large-area display technology developed by Samsung Display, characterized by a wide color gamut, excellent viewing angles, and high contrast ratios [1–5]. QD-OLED technology represents an evolution of existing display manufacturing, not only in terms of QD materials but also in terms of manufacturing processes and equipment with inkjet printing technology at its core. Prior to the development of QD-OLED displays, inkjet printing was used to produce organic thin films that formed organic/inorganic hybrid thin-film encapsulations (TFEs) in mobile displays [6–8]. In QD-OLED displays, however, inkjet printing technology has advanced to the point where it can produce QD pixels with fine patterns that directly contribute to light emission.

Although QD-OLED displays have introduced innovation in the manufacturing process through inkjet printing, it remains debatable whether they are more competitive than OLED and micro-LED displays [9–15]. Due to the characteristics of the QD material used as pixels, QD-OLEDs may be superior to OLEDs in terms of image quality, such as color gamut and viewing angle [1–5]. However, QD-OLEDs require more processes than existing OLED manufacturing methods because QD pixels with color conversion functionality are integrated into the blue (B) tandem OLED light source of the top-emitting structure. In addition, it has been reported that the cost advantage for television (TV) panels is

* Corresponding author.
E-mail address: bhwak@etri.re.kr (B.-H. Kwon).

https://doi.org/10.1016/j.cej.2026.177307
Received 10 January 2026; Received in revised form 22 March 2026; Accepted 12 May 2026
Available online 13 May 2026

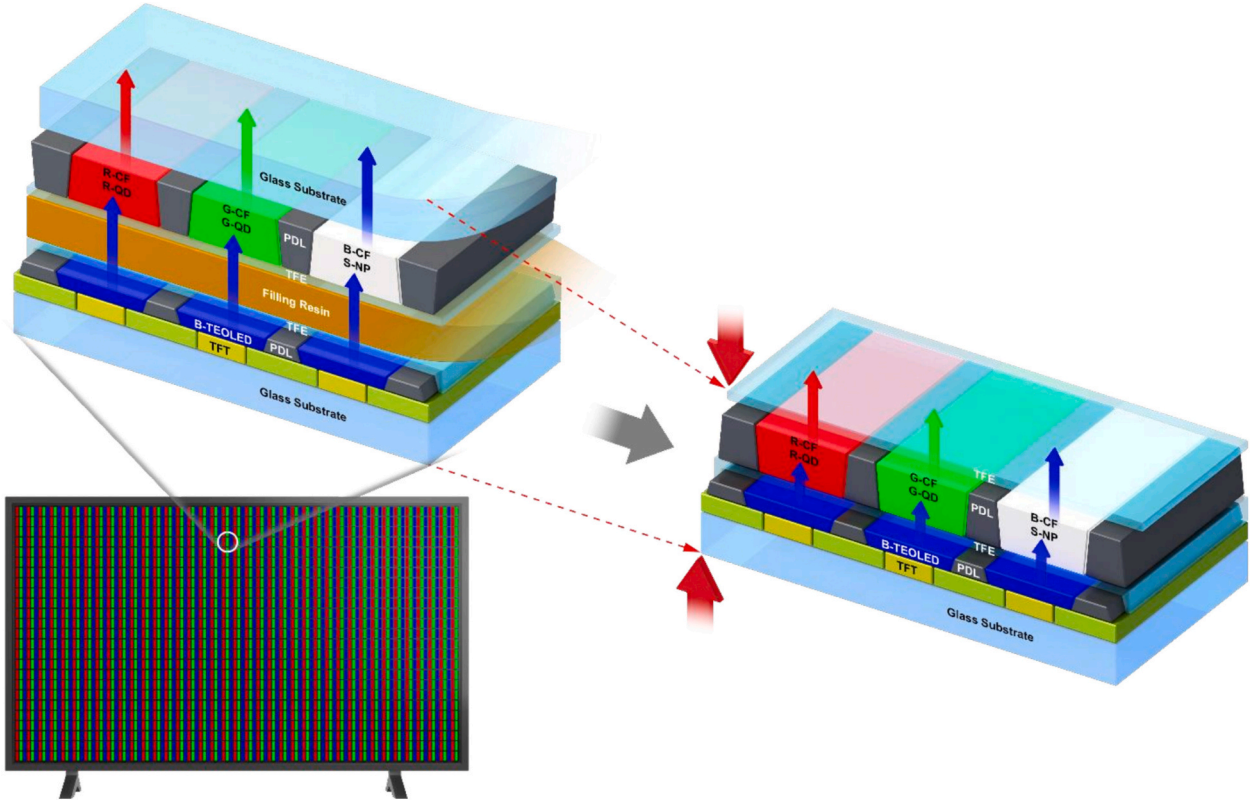

Fig. 1. Schematic comparison between a conventional quantum dot organic light-emitting diode (QD-OLED) structure fabricated using two glass substrates bonded with a filler resin and the proposed stacked QD-OLED structure fabricated on a single glass substrate with vertically integrated layers.

insignificant due to the additional investment required for new inkjet printing technology. Therefore, to establish QD-OLED displays as next-generation displays, new strengths must be added not only in terms of functionality, but also in terms of manufacturing process and cost.

In this study, a vertically stacked QD-OLED technology is presented that advances beyond current industrial QD-OLED displays. In current QD-OLED displays, a driver/OLED light source and QD pixels are manufactured on two glass substrates and then bonded together. In the vertically stacked QD-OLED display, the driver, OLED light source, and QD pixels are continuously manufactured on a single glass substrate. As a result, vertically stacked QD-OLEDs can reduce material costs and simplify the manufacturing process compared to existing QD-OLEDs. The recently commercialized color-filter-on-encapsulation OLED technology for mobile and foldable displays serves as a pertinent industrial reference. In the color-filter-on-encapsulation OLED structure, the polarizer is removed, and the TFE layer is formed on top of the OLED, followed by the fabrication of a black pixel-defining layer (PDL) and color filter (CF) at low temperature. This vertically stacked functional structure is used in commercial products because it reduces power consumption, increases optical transmittance, and improves cost efficiency [16]. In addition, the vertically stacked QD-OLED can incorporate a flexible or stretchable substrate in place of one glass substrate, allowing the display structure to be easily optimized. This makes it much easier to implement a freeform factor than an existing display with two substrates. In addition, existing QD-OLEDs incorporate a filler resin between the two substrates for bonding; however, the filler layer requires a thickness of tens of micrometers or more. Although this thickness is acceptable for TV-level resolution, it is difficult to apply the structure to high-resolution display devices such as mobile and mixed-reality devices due to optical interference effects [17–19]. In contrast, vertically stacked QD-OLEDs do not require a filler layer to bond the two substrates together, and the TFE thickness can be made sufficiently thin. Therefore, they are well-suited for a broad range of applications, including high-resolution micro displays, sensor-embedded displays, and TVs [17–26].

In addition, a novel technology for stacked QD-OLED panels was developed using printhead components and equipment compatible with mass-production processes in the display industry. The QD ink, TiO_2 nanoparticle (NP) ink, and black PDL material are all produced and applied in the display industry, confirming their industrial relevance and academic significance. Furthermore, in the stacked QD-OLED display, QD pixels were implemented on a top-emitting OLED (TEOLED) by introducing a low-temperature-cured black PDL material, which has not previously been used in the industry. By integrating these highly applicable component technologies, a QD-OLED panel consisting of 184,800 subpixels with a resolution of 141 pixels per inch (ppi), corresponding to a 65-inch 8K TV, can eventually be realized through a 6-inch substrate-based process.

2. Experimental methods

2.1. Materials

The QD inks for the green (G) and red (R) pixels, TiO_2 scattering-NP (S-NP) ink for the blue pixels, and CF material were all industrial-grade materials synthesized by CHEME Co., South Korea. The QD ink is a solvent-free composition consisting of indium phosphide (InP)-based core-shell structured QDs, photocurable monomers, photoinitiators, and functional additives (scattering agents, surfactants, adhesion promoters, etc.). The QD content in the ink was 30–35 wt%, and TiO_2 NPs (190–210 nm) were used as the scattering agent. The G-QDs exhibited a photoluminescence quantum yield (PL QY) in the range of 90–94%, while the R-QDs showed a PL QY of 92–97% in solution (Fig. S1). The black PDL photoresist for the QD pixels was synthesized by DUKSAN Neolux, Co., Ltd., South Korea.

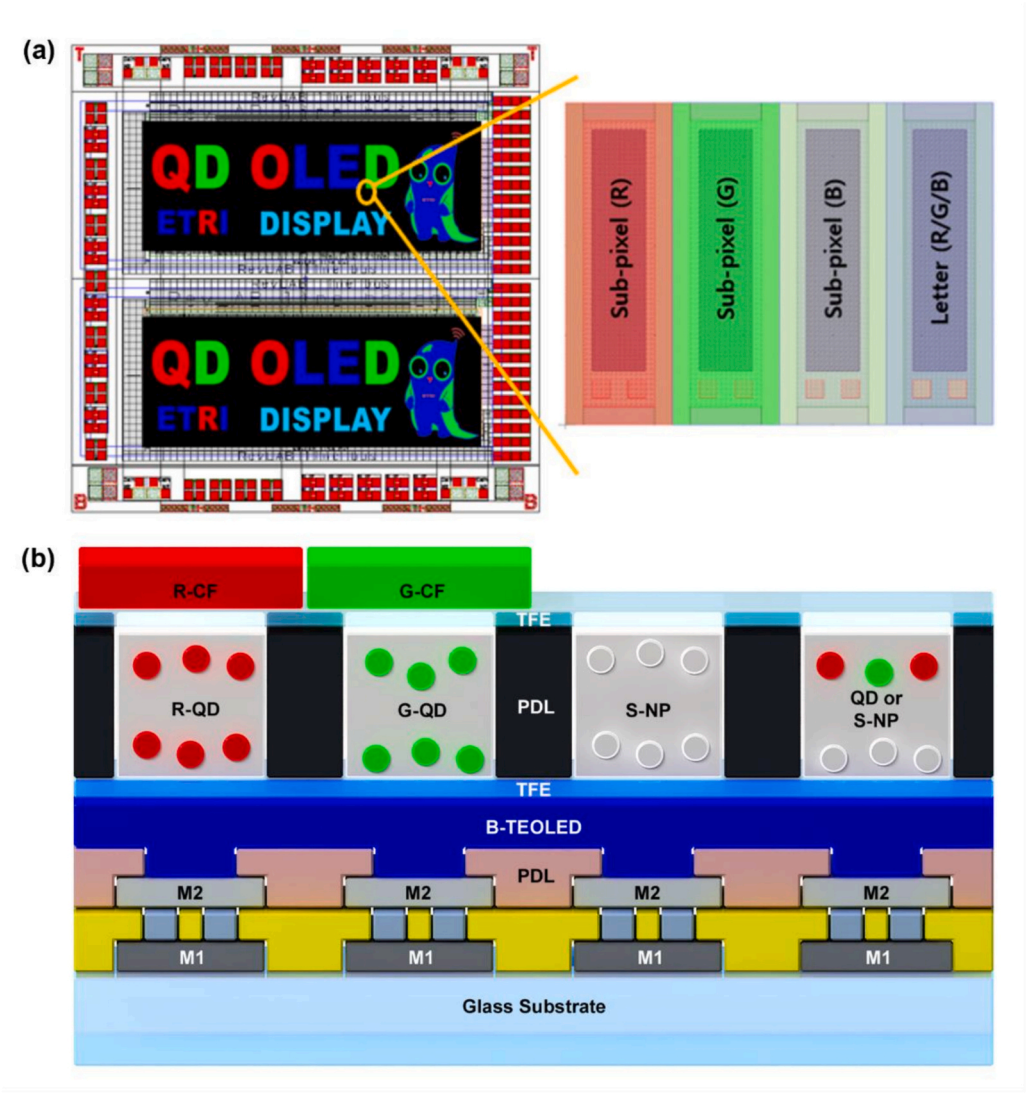

Fig. 2. (a) Schematic layout of the stacked quantum dot–organic light-emitting diode (QD-OLED) panel and pixel configuration. (b) Cross-sectional structure of the stacked QD-OLED panel showing the layer architecture.

2.2. Fabrication of stacked QD-OLED panel

The pixel structure was developed considering the size and resolution of TVs commercialized in the display industry, the structure of the black PDL, and the manufacturing process. The 65-inch 8K (7680 × 4320) TV was selected as the target, and the height (H) of a color conversion layer (CCL) was set to approximately 10 μm based on the QD color conversion efficiency (CCE) requirements. As a result, the subpixel width (W) and length (L) were set to 60 μm and 180 μm, respectively, in the QD unit pixel. Consequently, the stacked QD-OLED pixel size and the spacing (S) between PDLs were designed as 158.625 μm × 180 μm and 12.875 μm, respectively.

The stacked QD-OLED panel consisted of a TEOLED unit, TFE unit, black QD PDL unit, QD pixel unit, and CF unit. Each manufacturing process is described below. The pixel electrode of the panel consisted of double electrodes: an auxiliary electrode (M1) and a reflective electrode (M2). Following metal deposition on a glass substrate, the auxiliary electrodes were patterned using photolithography. For the reflective electrode, an insulating layer (SiO_2) was deposited on the auxiliary electrode, and a via hole was created using photolithography. The reflective electrode was then deposited and patterned using photolithography. All layers in the device were deposited by thermal evaporation under high vacuum at pressures in the range of 10^{-7}–10^{-8} Torr. The blue tandem TEOLED light unit of the top-emitting structure was fabricated as follows: Hole transport layer (HTL): P-type dopant (PD) (8.5 nm: 15%) as a hole injection layer (HIL) / HTL (140 nm) as an HTL / blue host (BH): blue dopant (BD) (20 nm: 6%) as an emitting layer (EML) / electron transport layer (ETL) (20 nm) / ETL: Li (20 nm: 5%) as an n-doped charge generation layer (n-CGL) / HTL: PD (8.5 nm: 15%) as a p-doped CGL(p-CGL) / HTL (60 nm)/ BH: BD (20 nm: 6%) as an EML/ ETL (30 nm) / Mg: LiF (1 nm: (1:1)) as an electron injection layer (EIL)/ Ag: Mg (15 nm: (8:2))/ capping layer (CPL) (80 nm) [27].

The TFE manufacturing process is as follows: Al_2O_3 and SiN_x were selected as TFE materials, and thin films of 90 and 600 nm were deposited using plasma-enhanced atomic layer deposition (PEALD) and plasma-enhanced chemical vapor deposition (PECVD), respectively. Trimethylaluminum (TMA) was used as the Al precursor. Argon (Ar) was used as the carrier and purging gas. The base pressure of the deposition chamber was ~10^{-3} Torr, and all layers were deposited at 95 °C. Subsequently, a SiN_x layer was deposited using silane (SiH_4) and ammonia (NH_3) as precursors [8,28–30]. PEALD was performed using thin-film passivation process equipment for flexible displays (TFPFD) [FEMC project]. The fabrication process for the black QD PDL was as follows. A black photoresist was spin-coated on the glass substrate to a thickness of

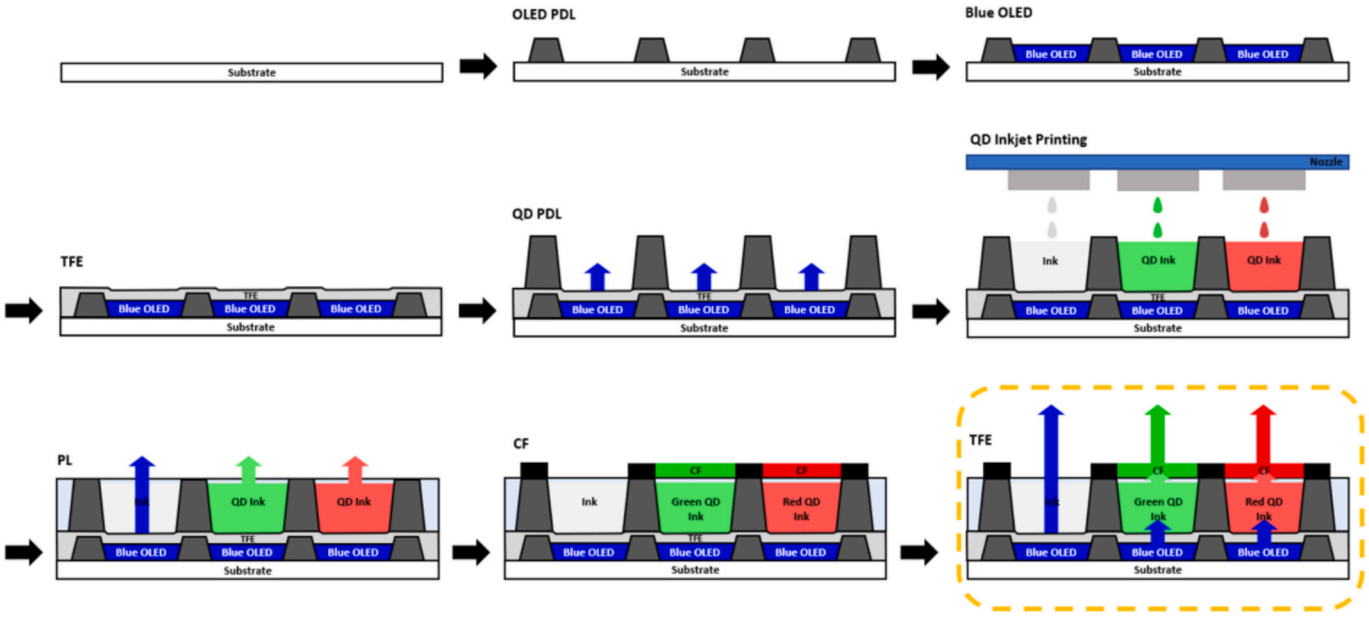

Fig. 3. Schematic illustration of the sequential fabrication process for the stacked quantum dot–organic light-emitting diode (QD-OLED) panel, including organic light-emitting diode (OLED) formation, thin-film encapsulation (TFE), black pixel-defining layer (PDL) fabrication, quantum dot (QD) inkjet printing, and color filter (CF) formation.

10 μm. The coated glass was soft-baked on a 100 °C hot plate for 100 s. The substrate was placed in the mask aligner, and the photoresist was irradiated with selective ultraviolet (UV) light. The substrate was developed with 0.04% potassium hydroxide (KOH) developer and subsequently rinsed with deionized water for 60 s. It was then hard-baked at 100 °C for 1 h in a convection oven. The QD printing process was as follows: inkjet printing was performed using an industrial printhead (KM-1024iSHE, 1024 nozzles, 360 DPI, 6 pL) from Konica Minolta Inc., Japan. Waveform conditions appropriate for the printhead were established. QD ink was printed through multiple nozzles of the printhead onto the PDL arrays. When UV light was irradiated onto the liquid ink, radicals generated from the photoinitiator induced a photopolymerization reaction of the monomers to form the film. Solidification was achieved solely through photocuring without a separate solvent volatilization process.

R and G CFs were fabricated using the following process: the R CF photoresist was spin-coated and prebaked at 100 °C. Exposure was performed using an i-line (365 nm) stepper, and the development process used a KOH spray gun. A post-bake at 100 °C completed the fabrication of the R CF, and the same process was repeated for the fabrication of the G CF [31].

2.3. Characterization

The current density–voltage–luminance (*J–V–L*) characteristics and the electroluminescence (EL) spectra were analyzed using a source-measure unit system (Keithley-238) and a spectroradiometer equipped with a goniometer (Model CS-2000, Konica Minolta). *J–V–L* measurements were performed at room temperature in a dark room. Efficiencies were calculated from the L, V, and EL spectra. Absorption and transmittance spectra were measured with a UV–visible (Vis)–near-infrared (NIR) spectrometer (PerkinElmer Lambda 750). The PL QY of the QDs used in this study was measured under blue light excitation at 450 nm. Scanning electron microscopy (SEM) images were obtained using an S-4800 microscope (Hitachi, Tokyo, Japan). A confocal fluorescence microscope (Carl Zeiss LSM880 with Airyscan) was used to obtain PL images of the printed QD pixel arrays. The rheological properties of the QD inks were characterized between 1 and 5000 Hz using a squeeze-flow rheometer (TriPAV, Trijet LIMITED). The temperature was maintained at 25 °C using an external thermo-circulator (PT80, KRÜSS) in conjunction with a thermometer (GMH3710, Greisinger). A lock-in amplifier (SR860, Stanford Research Systems) was used for signal acquisition and control of the piezo-axial vibration system.

3. Results and discussion

3.1. Description of stacked QD-OLED structure

Fig. 1(a) shows a schematic comparison between a conventional QD-OLED and the novel stacked QD-OLED structure. In a conventional QD-OLED, the OLED component, including the driving unit, and the color conversion pixel component, including the QD pixel, are formed on separate glass substrates. The two substrates are then bonded with a filler resin between them [1–5]. In contrast, the novel stacked QD-OLED is fabricated by first forming the OLED component, including the driving unit, on a glass substrate, followed by sequential deposition of the QD pixel component and protective layer. Unlike the conventional QD-OLED, the stacked QD-OLED eliminates the need for an additional filler layer for bonding to the upper substrate. This offers the advantage of reducing material consumption, simplifying the process, and significantly reducing the overall panel thickness. In particular, this structural differentiation plays a decisive role in suppressing optical crosstalk in high-resolution displays. In the case of conventional QD-OLED structures, the filler layer used to bond the two substrates typically has a thickness of tens of μm, which lengthens the optical path between the light source and the CCL, thereby intensifying interference phenomena where blue light scatters to QDs in adjacent pixels. In contrast, the stacked structure presented in this study minimizes light diffusion by removing the filler layer and applying a TFE layer of 1 μm or less, thereby drastically shortening the physical distance between the light source and the QD pixel compared to the conventional approach. Simulations have demonstrated that the effects of optical interference are nearly eliminated when the encapsulation layer thickness is controlled to within 1 μm in OLED on silicon displays at the 3000 ppi level [19]. Therefore, the stacked QD-OLED structure of this study demonstrates optical suitability for achieving high resolution and high image quality, and offers structural advantages that are highly favorable for mixed-reality display applications if photolithography or

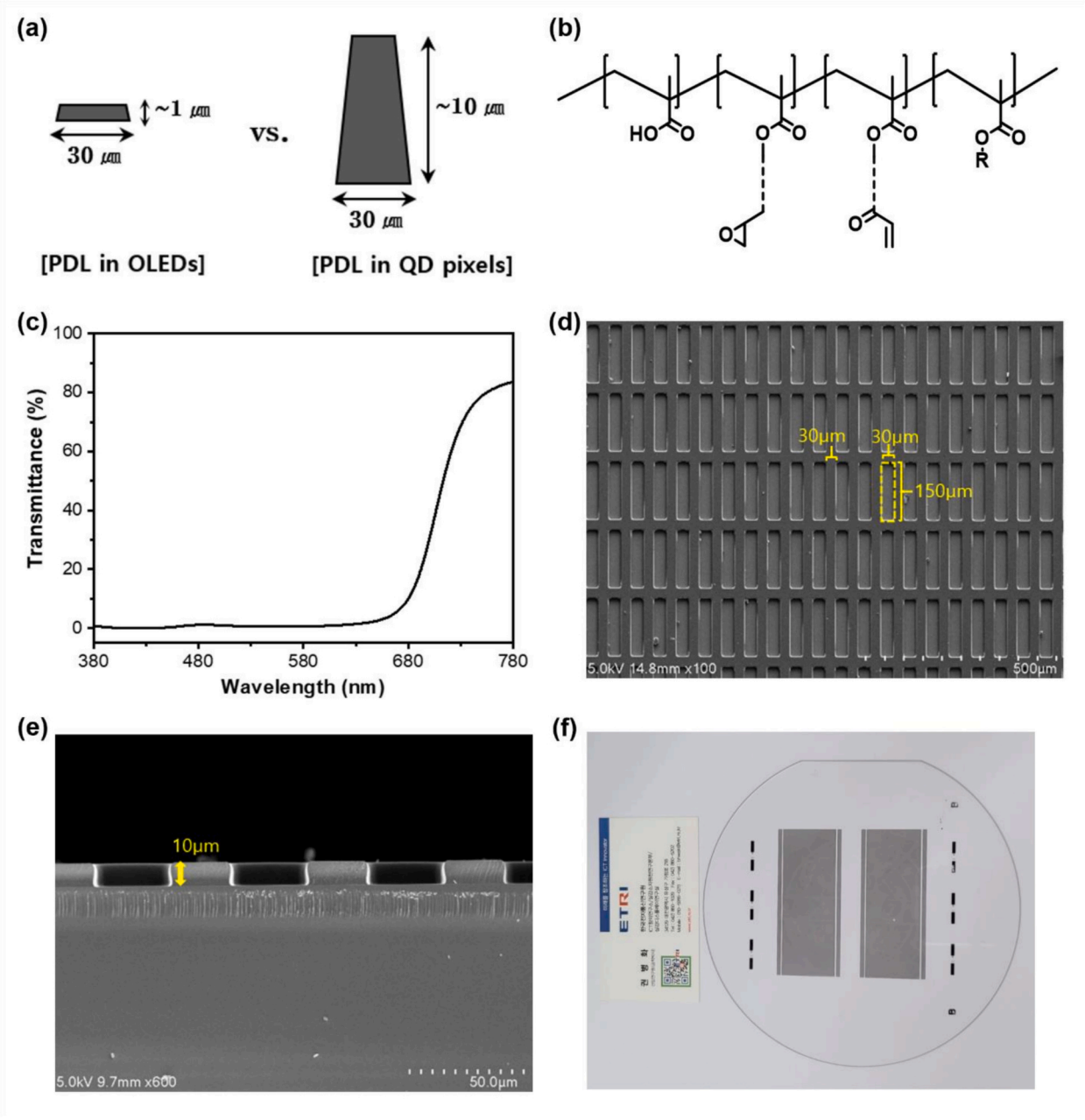

Fig. 4. (a) Schematic comparison of pixel-defining layer (PDL) structures in organic light-emitting diode (OLED) and quantum dot–organic light-emitting diode (QD-OLED) devices. (b) Chemical structure of the black PDL polymer. (c) Optical transmittance of the black PDL film. (d) Top-view and (e) cross-sectional scanning electron microscopy (SEM) images of the PDL arrays. (f) Photograph of PDL arrays fabricated on a 6-inch glass substrate.

electrohydrodynamic (EHD) printing processes are applied in the future.

Fig. 2 shows a schematic and structural cross-section of the stacked QD-OLED panel developed by the Electronics and Telecommunications Research Institute (ETRI) in the Republic of Korea. Fig. 2(a) shows a general schematic representation of the segmented panel developed on a 6-inch substrate and configured such that two panels are produced within an area of 100 mm × 100 mm. The pixel structure is shown next to the panel schematic. The RGB subpixels are responsible for conventional full-screen color display, whereas the letter (L) subpixel, a dedicated subpixel for displaying fixed text and graphic patterns, is used to display predefined content such as the "QD OLED ETRI DISPLAY" label and the "ETRI character" image implemented on the panel. The expected illumination image is also shown next to the panel schematic. The pixel arrangement in the display area of the panel is 330 × 140 comprising 46,200 pixels (330 × 140 × 4 = 184,800 subpixels).

Fig. 2(b) shows the structural cross-section of the stacked QD-OLED panel. The pixel electrode of the blue TEOLED panel uses a dual electrode, consisting of an auxiliary electrode and a reflective electrode, to lower the wiring resistance and reduce the resistive voltage drop. The Al_2O_3/SiN_x TFE structure was applied to the top of the blue OLED, and the QD pixel, which consists of the QD and black PDL, was positioned it was positioned above the TFE layer. In addition, a CF was formed on top of the QD pixel to remove blue light leakage.

Fig. 3 shows a schematic representation of the manufacturing process for the stacked QD-OLED panel. The core unit processes comprising the panel, namely blue TEOLED, TFE, black PDL, QD inkjet printing, and CF manufacturing, are performed continuously on a single glass substrate. For this type of continuous stacking process to succeed, the TFE structure must be robust enough to protect the underlying OLED device from damage during the photolithography and inkjet printing processes

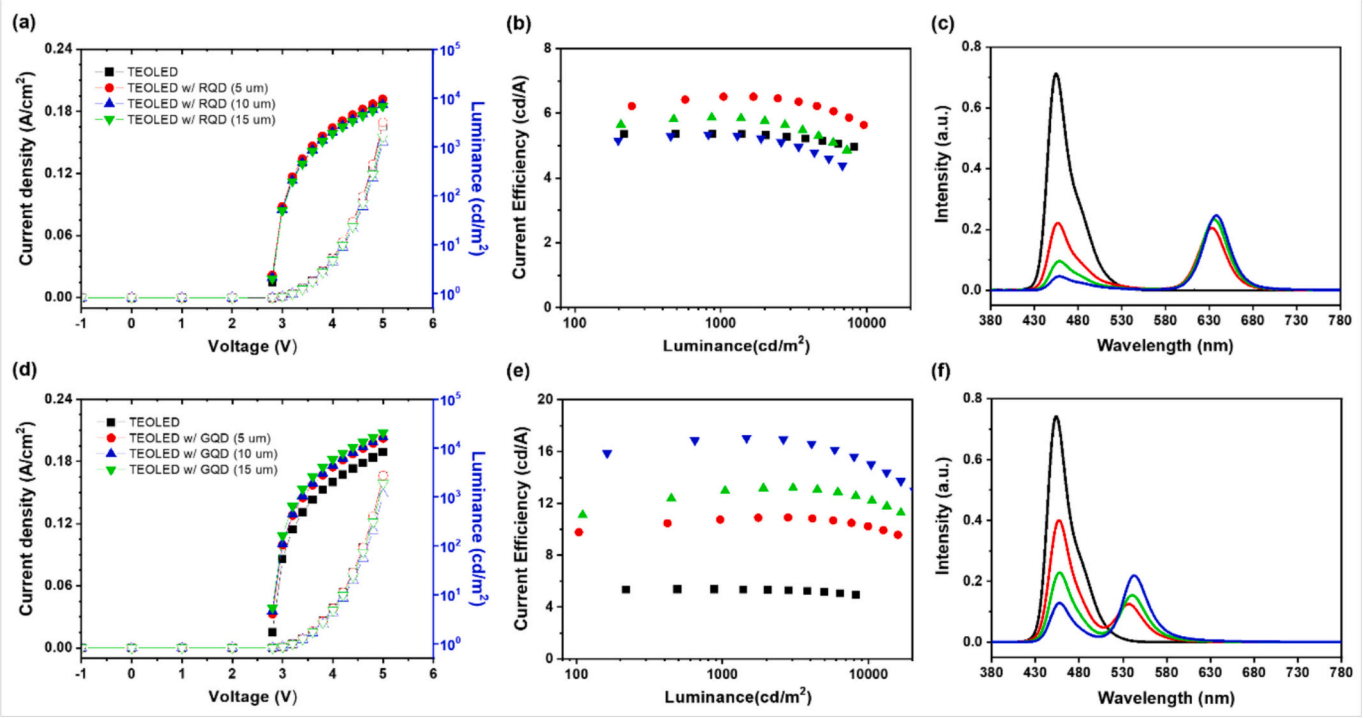

Fig. 5. (a) Current density–voltage–luminance (J–V–L) characteristics, (b) current efficiency–luminance characteristics, and (c) electroluminescence (EL) spectra of devices with red quantum dot (QD) color conversion layers (CCLs) of 5, 10, and 15 μm thickness formed on blue top-emitting organic light-emitting diodes (TEOLEDs). (d–f) Corresponding J–V–L characteristics, current efficiency, and EL spectra for devices with green QD CCLs of varying thickness.

Table 1
Summary of luminance, current efficiency, CCE, and output-to-input photon ratio of device with R-QD and G-QD CCL formed on blue TEOLED.

	Luminance (cd/m^2)	Current efficiency (cd/A)	CCE (%)	Output-to-input photon ratio (%)
TEOLED	2038.3	5.3	–	–
TEOLED with R-QD (5 μm)	2460.7	6.5	46.7	31.5
TEOLED with R-QD (10 μm)	2002.3	5.8	41.6	35.4
TEOLED with R-QD (15 μm)	1888.2	5.2	40.3	37.3
TEOLED with G-QD (5 μm)	4126.6	10.8	41.9	20.1
TEOLED with G-QD (10 μm)	4465.8	13.1	33.4	23.6
TEOLED with G-QD (15 μm)	5868.0	16.1	38.4	32.3

used to produce the QD pixels. In addition, the process temperature for fabricating the black PDL of the QD pixel must remain below 100 °C to avoid degradation of OLED performance.

3.2. Characteristics of black PDL patterns

Fig. 4 presents the characterization results of the black QD PDL, which confines the printed QD ink within defined pixel wells. Fig. 4(a) shows the structure of the PDL used for the QD pixels in the QD-OLED and the OLED. The height of the PDL in the OLED is approximately 2–3 μm, while in the QD-OLED it is considerably thicker, at approximately 8–10 μm. This difference is related to the color conversion requirements of the QD layer, as a greater CCL thickness is necessary to achieve sufficient QD CCE. In addition, the PDL of the QD-OLED enables well-defined pixel geometries when the taper angle is approximately 80°. Most critically, to fabricate the black PDL on the TFE of the tandem TEOLED for the realization of stacked QD-OLEDs, it is essential to use a material that can be cured at temperatures below 100 °C without damaging the underlying OLED. The PDL currently used in the display industry requires a high thermal curing temperature of approximately 250 °C. However, in this study, a black PDL material processable at temperatures at or below 100 °C was developed and utilized. The black PDL material is composed of black pigment, a polymer binder, a, photoinitiator, monomer, and solvent; the polymer structure used in this study is shown in Fig. 4(b) [16,32,33]. In this structure, acrylate groups were incorporated into the side chains of the acrylic polymer backbone to increase crosslinking density and improve photoreactivity, while epoxy groups were introduced to enhance thermal reliability. In addition, a photoinitiator with high absorption at the i-line wavelength (365 nm) used for photolithographic exposure was incorporated into the black PDL formulation (Fig. S2). This photoinitiator enables efficient radical generation through strong UV absorption at 365 nm, facilitating adequate crosslinking even under reduced thermal budgets. Fig. 4(c) shows the optical transmittance spectra of the black PDL in the QD unit pixel. The thickness of the black PDL was set to approximately 10 μm based on the color conversion requirements of the CCL. The transmittance at 450, 550, and 650 nm was 0.26%, 0.62%, and 2.52%, respectively. This confirms that the black PDL material has suitable optical properties for application in QD-OLEDs. Fig. 4(d) and (e) show SEM images of the micropatterned PDL array. The number of subpixels formed by the black PDL array was 3025 (55 × 55). The PDL dimensions are 30 μm for W and S, 150 μm for L, and 10 μm for H. This confirms that all PDLs were uniformly produced with consistent dimensions. The adhesion between the black PDL and the underlying layer was controlled through photolithographic exposure conditions, particularly the

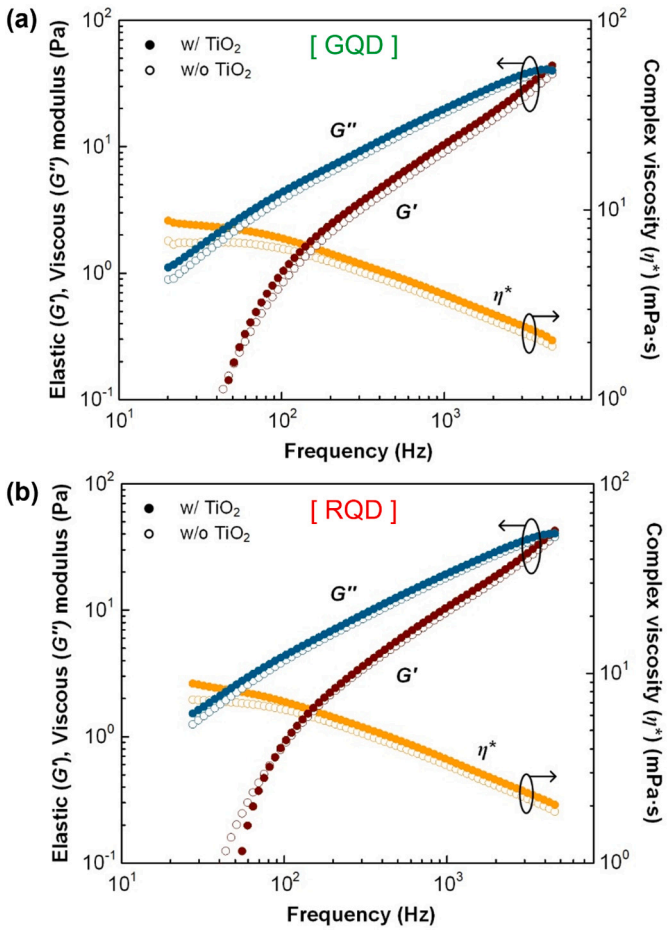

Fig. 6. Rheological characterization of quantum dot (QD) inks, showing frequency-dependent viscoelastic properties relevant to inkjet printing performance.

exposure time. When an insufficient exposure time of 3 s was used, distorted black PDL patterns and partial delamination from the substrate were observed. In contrast, an exposure time of 5 s resulted in sufficient curing throughout the black PDL thickness, improving pattern integrity and increasing adhesion to the substrate, as shown in Fig. S3. Fig. 4(f) shows a photograph of the PDL fabricated on a 6-inch glass substrate. This result demonstrates process uniformity across a large-area substrate.

3.3. QD color conversion and rheological properties

The color conversion properties of the QD ink for inkjet printing were evaluated under illumination from the OLED light source. R and G QD films with thicknesses of approximately 5, 10, and 15 μm were formed on the TEOLED encapsulation layer. Figs. 5(a)–(c) show the *J–V–L* characteristics, current efficiency, and EL spectra of the TEOLED device incorporating the R-QD CCL. The device with R-QD CCL exhibited diode-like J-V characteristics similar to those of the device without CCL, indicating that formation of the QD layer did not affect the electrical stability of the underlying TEOLED device. Specifically, at 4.0 V, the device without QD CCL and the R-QD CCL devices with thicknesses of 5, 10, and 15 μm recorded luminance values of 2038.3, 2460.7, 2002.3, and 1888.2 cd/m^2, respectively. The current efficiencies at the corresponding luminance levels were measured to be 5.3, 6.5, 5.8, and 5.2 cd/A, respectively. Analysis of the emission spectra revealed that as the R-CCL thickness increased, the blue emission peak (455 nm) decreased and the R emission peak (637 nm) increased, suggesting that the QD CCL effectively converted the blue TEOLED emission. Figs. 5(d)–(f) show the properties of the TEOLED device incorporating the G-QD CCL. Similar to the R-QD CCL device, the G-QD CCL device exhibited stable behavior and displayed high luminance values of 4126.6, 4465.8, and 5868.0 cd/m^2 at thicknesses of 5, 10, and 15 μm, respectively, at 4.0 V. The current efficiencies at the corresponding luminance levels were 10.8, 13.1, and 16.1 cd/A, respectively. Efficient color conversion was further confirmed by the proportional increase in R emission intensity (542 nm) with increasing film thickness.

The CCE and output-to-input photon ratio were calculated according to the reported formula, and the corresponding values are summarized in Table 1 [34–39].

TEOLED, top-emitting organic light-emitting diode; QD, quantum dot; CCL, color conversion layer; R-QD, red quantum dot; G-QD, green quantum dot; CCE, color conversion efficiency. — indicates that the metric is not applicable for the bare TEOLED reference device.

The CCEs of devices using R-QD CCL with thicknesses of 5, 10, and 15 μm were 46.7%, 41.6%, and 40.3%, respectively, while those of G-QD CCL devices were 41.9%, 33.4%, and 38.4%. In a study published by Nanosys, Inc., a leading QD manufacturer, InP QD thin films thinner than 10 μm were shown to exhibit CCE values exceeding 38% for R and 30% for G under a 450 nm blue LED light source [36]. In the present study, using a 455 nm blue OLED light source, CCE values exceeding 41.6% for R and 33.4% for G were achieved at InP QD thin film thicknesses below 10 μm. This demonstrates that the material developed in

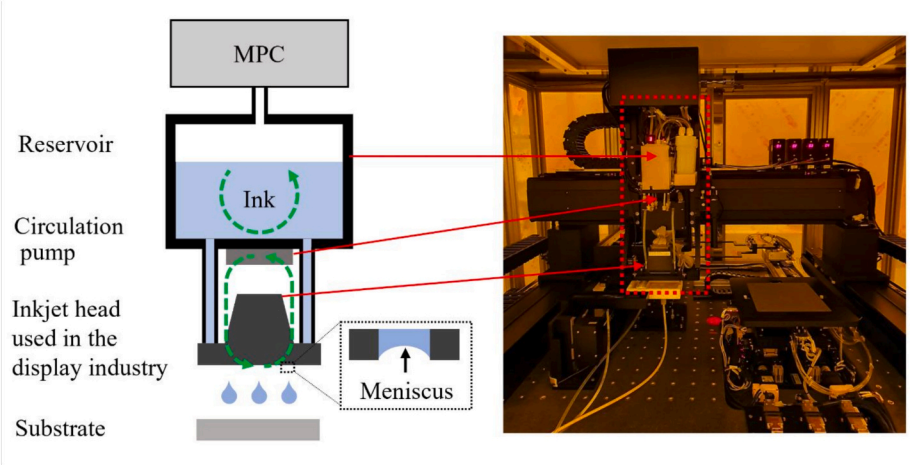

Fig. 7. Schematic of the inkjet head module illustrating ink circulation and meniscus formation at the nozzle, along with a photograph of the industrial inkjet printing system used in this study.

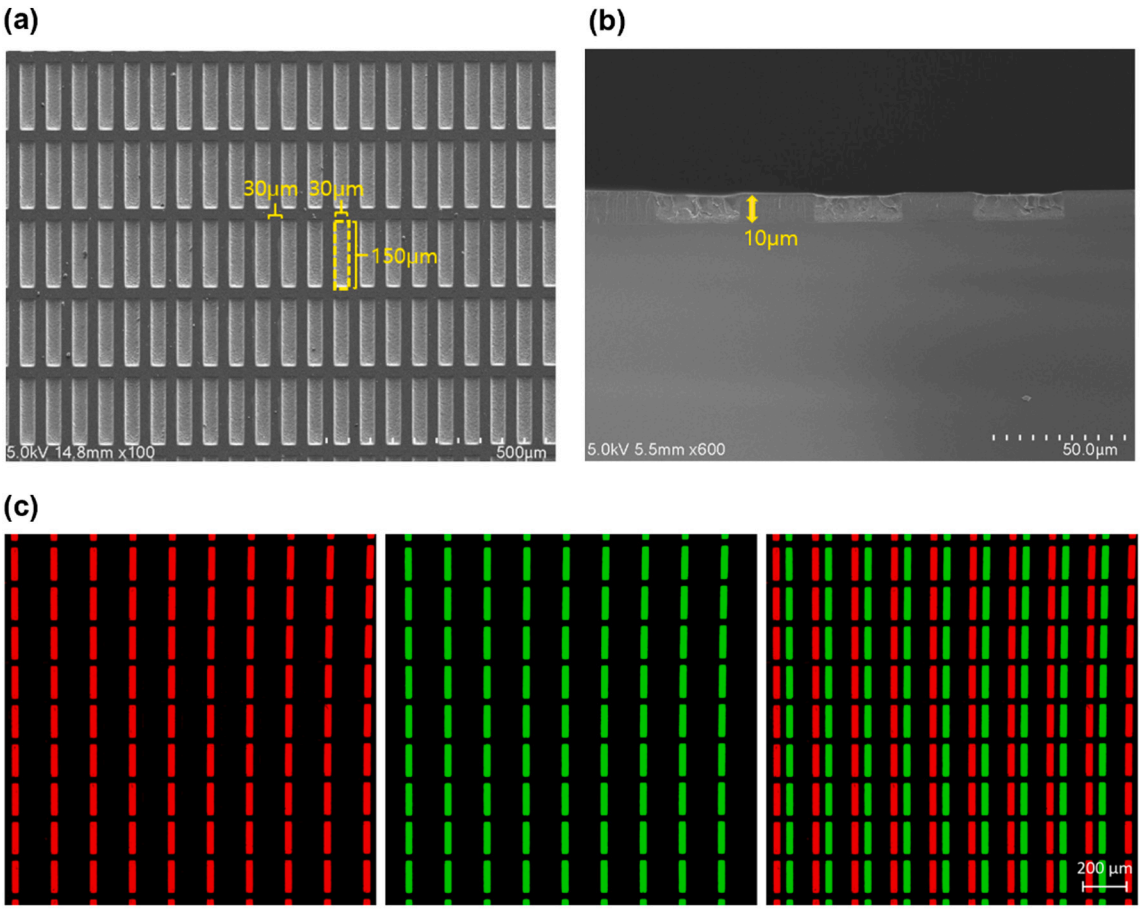

Fig. 8. (a) Top-view and (b) cross-sectional scanning electron microscopy (SEM) images of quantum dot (QD) subpixels fabricated by filling black pixel-defining layer (PDL) arrays with QD ink. (c) Fluorescence image of patterned QD subpixels formed by sequential deposition of red (R) and green (G) QDs using inkjet printing.

this study possesses superior optical properties compared to prior art and meets the performance requirements for practical display industry applications.

A phenomenon termed “blue light leakage” was observed, in which some blue light was transmitted without being fully converted as it passed through the QD layer. This leakage decreased as the optical absorption path length increased with film thickness. However, while it is theoretically possible to maximize color purity by forming the QD pixel layer sufficiently thick, the thickness of the black PDL, which suppresses optical crosstalk between pixels, must increase proportionally, imposing additional process constraints. Increased black PDL thickness narrows the process window, making it more challenging to achieve sufficient exposure depth and maintain pattern precision at high-aspect-ratio geometries during photolithography. To overcome these process constraints and effectively suppress blue light leakage, this study investigated the effect of incorporating S-NPs into the QD ink. As shown in Fig. S7, the addition of S-NPs extended the optical path length within the QD layer, thereby reducing blue light leakage while simultaneously improving CCE. Therefore, given the difficulty of maintaining adequate process margins and the cost of material optimization, the display industry currently achieves the required color purity by depositing a CF on top of the QD pixel layer, consistent with commercialized QD-OLED structures [10,11].

To assess the inkjet printability of the QD inks, their rheological properties were investigated using a piezoelectric axial vibrator-based squeeze-flow rheometer. In particular, this instrument was used to measure the viscoelasticity of the inks at frequencies up to 5000 Hz, as the high-frequency response is particularly relevant to the fluid behavior at the inkjet nozzle during jetting [40,41]. As shown in Fig. 6, the QD inks exhibited weak shear-thinning behavior with a complex viscosity that decreased with frequency. Despite the extremely low complex viscosity at high frequencies, the significantly increased elastic modulus enabled reliable jet formation. The measurements also showed that the addition of TiO_2 had a negligible effect on viscoelasticity, causing only a small increase in complex viscosity and viscoelastic moduli. These results indicate that the ink formulation maintained stable rheological properties suitable for consistent and precise inkjet printing performance.

3.4. Fabrication of QD pixels using an industrial inkjet printing process

Fig. 7 shows a schematic representation of the inkjet head module for the QD materials, featuring precise pressure control and ink circulation functions. The inkjet head module consists of a meniscus pressure controller (MPC), a reservoir, and a printhead. The MPC controls the pressure inside the reservoir, which in turn regulates the ink supply. The printhead is responsible for ejecting ink droplets to the desired location. When the MPC controls the pressure, a uniform negative pressure is maintained inside the reservoir. The negative pressure draws ink toward the printhead, preventing it from dripping from the nozzle under gravity [7,8,42,43]. Because the negative pressure governs the meniscus shape, the reservoir pressure must remain uniform. Unstable pressure control cannot maintain a constant meniscus, leading to inconsistent droplet ejection and poor print quality. Additionally, QD ink particles may sediment at the bottom of the reservoir or within the printhead. Such deposits result in nozzle clogging and print defects. To prevent sedimentation, the ink was stirred inside the reservoir and circulated along the conduit between the reservoir and the printhead. Continuous stirring

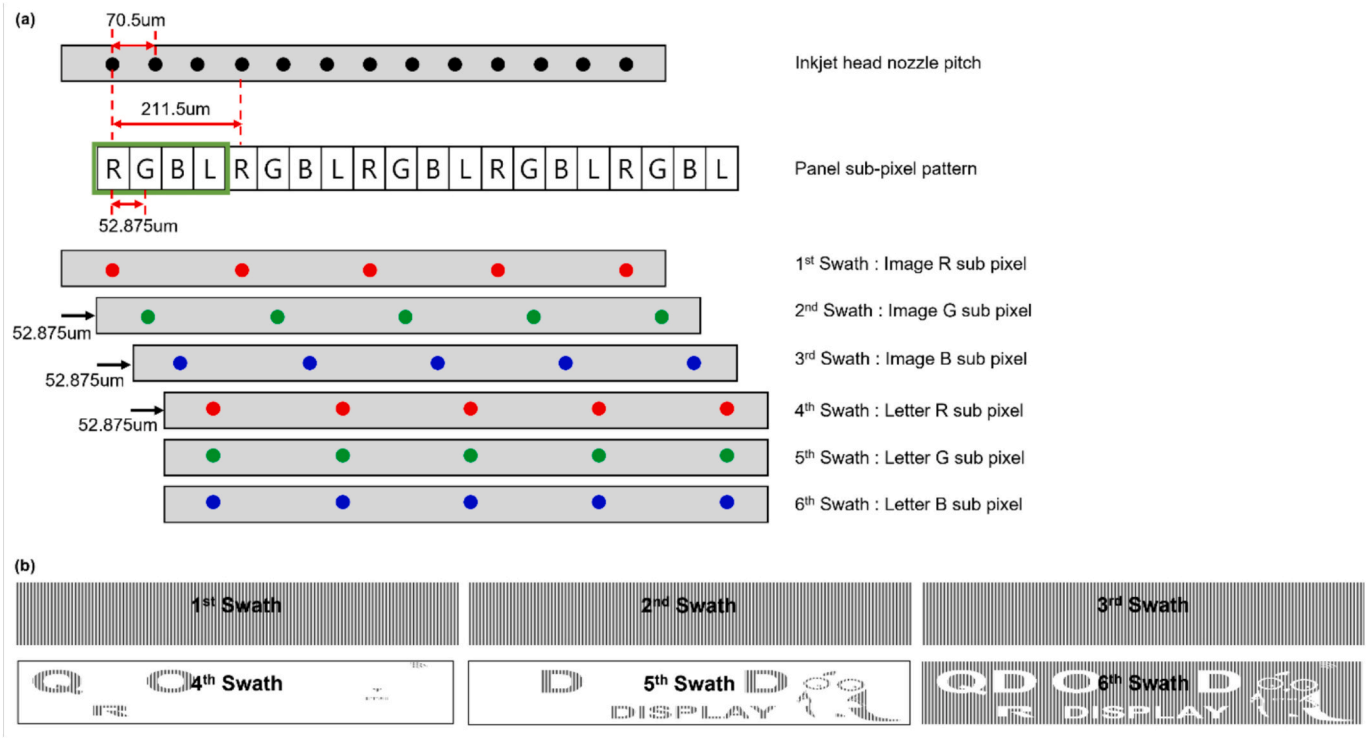

Fig. 9. Schematic illustration of quantum dot (QD) pixel fabrication in stacked quantum dot organic light-emitting diode (QD-OLED) panels using an industrial inkjet printhead, including subpixel arrangement and multi-pass (swath) printing strategy.

and circulation prevented sedimentation, eliminating nozzle clogging even with particle-laden inks. The Fig. 7 image shows the inkjet printing equipment installed at ETRI.

Fig. 8 shows the results of fabricating a 55 × 55 QD pixel array that mimics the RGB stripe pixel structure of a QD-OLED display on a unit substrate. The pixel is divided into a non-emitting region (black PDL structure) and an emitting region (TiO_2 or QD structure). The pixel size on the unit substrate was 180 × 180 μm, and H (pixel height) was 10 μm. The subpixel size was 60 × 180 μm, and S (spacing) was 30 μm. To suppress ink droplet overflow from the PDL, the surface energy of the black PDL was tuned by controlling the CF_4 plasma treatment conditions [35]. Without plasma treatment, the water contact angle of the black PDL surface was approximately 60°, whereas CF_4/O_2 plasma treatment increased the contact angle to approximately 90° (Fig. S4). These results confirm that CF_4 plasma treatment enables effective control of the surface energy of the black PDL. Figs. 8(a) and 8(b) show SEM plan-view and cross-sectional images of the subpixel formed by filling the black PDL wells with TiO_2 ink. The SEM images confirm that the ink was uniformly filled and cured within the PDL. Fig. 8(c) shows a fluorescence image of the pixel prepared by sequentially filling the PDL wells with alternating R and G QDs. The ink was selectively confined within the subpixel wells without overflowing onto the PDL surfaces. The blue subpixels were produced directly by the B emission of the TEOLED without a QD CCL; therefore, no blue fluorescence was observed in the image.

3.5. Development of stacked QD-OLED panels

Fig. 9(a) illustrates the inkjet printing process on the RGB and L subpixels of a stacked QD-OLED panel using an industrial printhead. The upper schematic shows a representation of the printhead (360 DPI) with nozzles spaced at 70.5 μm intervals. The lower schematic illustrates the panel pixel layout, with an L subpixel added alongside the RGB subpixels. If the RGB subpixels are formed based on the nozzle interval of 70.5 μm of the printhead, a pixel pitch of 211.5 μm can be achieved. However, in this panel, an L subpixel was added to the RGB subpixels, and four subpixels were accommodated within the 211.5 μm pixel pitch. Accordingly, each of the four RGBL subpixels measured 52.875 × 180 μm, with a spacing (S) of 12.875 μm. The lower image in Fig. 9(a) shows the inkjet printing process on the panel. To print one swath for each color, the inkjet process must match the pixel and nozzle spacing [6,7]. As with the RGB subpixels, each subpixel occupied its own designated area, and printing was performed by offsetting the printhead position by 52.875 μm to align with the R, G, and B subpixel positions. Therefore, the R, G, and B subpixels were produced in three swaths. The L subpixel must contain one of the colors, R, G, or B, depending on the design. Accordingly, the printhead deposited ink at the same position while the operating program was adjusted according to the target letter color. The RGB and L subpixels were each printed in three separate passes (R, G, and B), completing pixel fabrication in a total of six printing operations. Fig. 9(b) shows the printing pattern areas for the six swath prints. In swaths 1–3, the R-QD, G-QD, and TiO_2 NP inks were printed on the R, G, and B subpixels, respectively. In swaths 4–6, the R-QD, G-QD, and TiO_2 NP inks were then printed on the L subpixel in that order.

Fig. 10(a) shows the SEM images of the stacked QD-OLED panel. The SEM plan-view and cross-sectional images (upper left and upper right) show that the R, G, B, and L subpixels comprising the panel were uniformly arranged. R and G CFs were present on the R and G subpixels, whereas the B and L subpixels had no CFs. The high-magnification SEM cross-sectional views (lower left and lower right) show the OLED, black PDL, QD, and CF regions comprising the panel. The OLED region was a multilayer structure in which the electrodes, organic materials, and TFE layers are stacked sequentially. A magnified SEM image of the corresponding region is shown in Fig. S5. The lower electrode, consisting of $Mo/SiO_2/Mo/ITO$ (100/250/80/20 nm) on a glass substrate, was clearly visible. The region approximately 400 nm above the lower electrode was composed of multilayer organic materials and electrodes forming the TEOLED. In addition, the TFE Al_2O_3/SiN_x layer (90/600 nm) was clearly visible, with the QD PDL confirmed to have been deposited on top. Fig. 10(b) shows a photograph of the stacked QD-

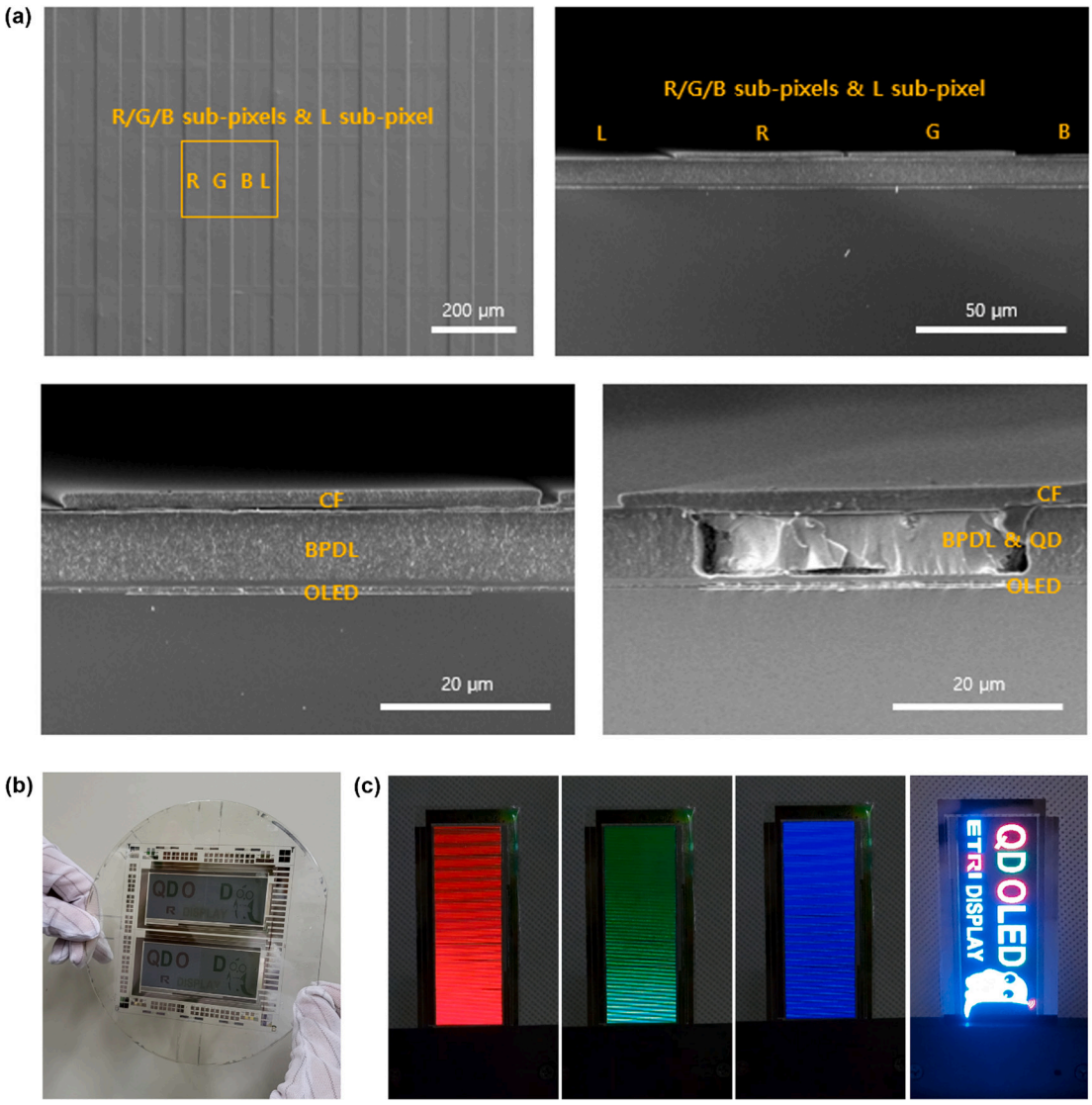

Fig. 10. (a) Scanning electron microscopy (SEM) images showing the plan-view and cross-sectional structure of the stacked quantum dot organic light-emitting diode (QD-OLED) panel. (b) Photograph of the fabricated panel on a 6-inch glass substrate. (c) Images of panel operation demonstrating individual red, green, and blue (RGB) subpixel emission and combined illumination.

OLED panel fabricated on a 6-inch glass substrate, in which some of the panel's text and graphic patterns are visible as reflections. The final display panel was completed through sequential vacuum deposition for the OLED layers, followed by photolithography and inkjet printing for QD pixel fabrication. Fig. 10(c) shows photographs of the panel under two illumination conditions: one in which the R, G, and B subpixels are illuminated individually, and one in which the L subpixels displaying R, G, and B emission are illuminated simultaneously. The corresponding videos are provided as Supplementary Information. Thus, a novel stacked QD-OLED panel featuring 184,800 QD subpixels integrated on a TEOLED has been successfully fabricated, illuminated, and demonstrated to operate stably.

4. Conclusion

In this study, a novel stacked QD-OLED panel with a structure superior to existing commercial QD-OLED displays was developed and reported for the first time. Stacked QD-OLED panels are more cost-competitive than existing QD-OLED panels because all fabrication processes, including TFT, OLED, and QD pixel layer, are performed sequentially on a single substrate. In addition, this approach is well suited for various substrates, such as flexible and stretchable substrates, and effectively reduces optical interference in high-resolution displays, positioning the stacked QD-OLED as a core technology for next-generation display development. The stacked QD-OLED panel demonstrated a resolution of 141 ppi, equivalent to that of a 65-inch 8K TV, with a total of 184,800 QD subpixels successfully fabricated using an inkjet printing process. The fabrication of QD pixels for the stacked QD-OLED was demonstrated using QD ink, a black PDL photoresist, and inkjet printing equipment suited for the display industry. First, a high-aspect-ratio black PDL processable at temperatures below 100 °C was fabricated via photolithography, and the resulting high-resolution PDL patterns were characterized. Next, the rheological properties of the QD ink were evaluated using a squeeze-flow rheometer, and the color conversion characteristics of the R- and G-QD CCL under a blue tandem TEOLED light source were analyzed. Finally, a technology was developed to form QD pixels on a blue tandem OLED panel using an industrial inkjet printhead, and stable panel operation was demonstrated. This stacked QD-OLED technology is expected to serve as a key enabler for the development of next-generation OLED on silicon and micro-LED displays incorporating QD materials across a broad range of form factors.

CRediT authorship contribution statement

Byoung-Hwa Kwon: Writing – review & editing, Writing – original draft, Validation, Supervision, Methodology, Investigation, Funding acquisition, Formal analysis, Data curation, Conceptualization. **Jin-Wook Shin:** Validation, Investigation, Formal analysis, Data curation. **Chul Woong Joo:** Validation, Investigation, Formal analysis, Data curation. **Chan-mo Kang:** Validation, Investigation, Formal analysis, Data curation. **Hyunsu Cho:** Validation, Investigation, Formal analysis, Data curation. **Sukyung Choi:** Validation, Investigation, Formal analysis, Data curation. **Yoonsung Yoo:** Validation, Investigation, Formal analysis, Data curation. **Hyungwoo Suh:** Validation, Investigation, Formal analysis, Data curation. **Dong-Kyun Shin:** Writing – review & editing, Writing – original draft, Validation, Data curation. **Jaeryul Yu:** Writing – review & editing, Writing – original draft, Validation, Data curation. **Yeon Soo Lee:** Validation, Methodology, Data curation. **Seongju Kim:** Writing – review & editing, Writing – original draft, Validation, Data curation. **Sungjune Jung:** Writing – review & editing, Writing – original draft, Validation, Data curation. **Chun Sakong:** Validation, Methodology. **Chun-Won Byun:** Validation. **Nam Sung Cho:** Validation.

Declaration of Generative AI and AI-assisted technologies in the writing process

N/A

Funding sources

N/A

Declaration of competing interest

The authors declare that they have no known competing financial interests or personal relationships that could have appeared to influence the work reported in this paper.

Acknowledgments

This study was supported by the ITECH R&D program of MOTIE/KEIT (project No. 20012560, Development of Material, Component, and Equipment for Inkjet Printing in Flexible QD-OLED) and an Electronics and Telecommunications Research Institute (ETRI) grant funded by the Korean government [26ZC1200, Research on Ultra-Realistic Spatial Device Technology]. The authors thank Editage (www.editage.co.kr) for English language editing.

Appendix A. Supplementary data

Supplementary data to this article can be found online at https://doi.org/10.1016/j.cej.2026.177307.

Data availability

Data will be made available on request.

References

[1] J.H. Lee, QD display: a game-changing technology for the display industry, Inf. Disp. 36 (2020) 9–13, https://doi.org/10.1002/msid.1163.
[2] C. Han, S. Lee, Y. Ko, J. Cho, Y.K. Jung, D.J. Kang, D. Kwak, S. Kim, J. Ha, Y.-G. Yoon, C. Lee, Inkjet-printed quantum dot light-emitting diodes: development and challenges for display applications, J. Soc. Inf. Disp. 33 (2025) 53–65, https://doi.org/10.1002/jsid.2006.
[3] D.J. Kang, D.-H. Lee, S. Jeong, E.-A. Yang, J. Park, Y.-G. Kim, J. Park, D. Kwak, S. Kim, H. Kang, T. Masanobu, Y.-G. Yoon, C. Lee, Controlling rheological properties of inks for developing high-resolution 264 ppi all inkjet-printed QD-LED display, J. Soc. Inf. Disp. (2025), https://doi.org/10.1002/jsid.2083.
[4] J. Kim, J. Roh, M. Park, C. Lee, Recent advances and challenges of colloidal quantum dot light-emitting diodes for display applications, Adv. Mater. 36 (2024) 2212220, https://doi.org/10.1002/adma.202212220.
[5] Z. Hu, Y. Yin, M.U. Ali, W. Peng, S. Zhang, D. Li, T. Zou, Y. Li, S. Jiao, S.-J. Chen, C.-Y. Lee, H. Meng, H. Zhou, Inkjet printed uniform quantum dots as color conversion layers for full-color OLED displays, Nanoscale 12 (2020) 2103–2110, https://doi.org/10.1039/C9NR09086J.
[6] V. Steinmann, L. Moro, Encapsulation requirements to enable stable organic ultra-thin and stretchable devices, J. Mater. Res. 33 (2018) 1925–1936, https://doi.org/10.1557/jmr.2018.194.
[7] K.-S. Kwon, M.K. Rahman, T.H. Phung, S.D. Hoath, S. Jeong, J.S. Kim, Review of digital printing technologies for electronic materials, Flex. Print. Electron. 5 (2020) 043003, https://doi.org/10.1088/2058-8585/abc8ca.
[8] B.-H. Kwon, C.W. Joo, H. Cho, C.-M. Kang, J.-H. Yang, J.-W. Shin, G.H. Kim, S. Choi, S. Nam, K. Kim, C.-W. Byun, N.S. Cho, S. Kim, Organic/inorganic hybrid thin-film encapsulation using inkjet printing and PEALD for industrial large-area process suitability and flexible OLED application, ACS Appl. Mater. Interfaces 13 (2021) 55391–55402, https://doi.org/10.1021/acsami.1c12253.
[9] Z. Xiao, M. Zhang, Y. Ding, Z. Shi, Z. Yin, H. Deng, L. Meng, B. Xu, H. Liu, Solution-processed quantum dot micropatterns: from liquid manipulation to high-performance quantum dot light-emitting diode devices, ACS Nano 19 (2025) 10609–10619, https://doi.org/10.1021/acsnano.5c01172.
[10] J. Burschka, C.-S. Choi, N. Greinert, E. Kossoy, T. Suzuki, A. Yamamoto, I. Koehler, Challenges in QD–OLED display technology, SID Symp. Dig. Tech. Pap. 53 (2022) 295–298, https://doi.org/10.1002/sdtp.15478.
[11] G. Li, M.-C. Tseng, Y. Chen, F.S.-Y. Yeung, H. He, Y. Cheng, J. Cai, E. Chen, H.-S. Kwok, Color-conversion displays: current status and future outlook, Light Sci. Appl. 13 (2024) 301, https://doi.org/10.1038/s41377-024-01618-8.
[12] J. Shin, H. Kim, S. Sundaram, J. Jeong, B.-I. Park, C.S. Chang, J. Choi, T. Kim, K. Saravanapavanantham, S. Lu, J.M. Kim, K.S. Suh, M.-K. Kim, Y. Song, K. Liu, J. Qiao, J.H. Kim, Y. Kim, J.-H. Kang, J. Kim, D. Lee, J. Lee, J.S. Kim, H.E. Lee, H. S. Yeon, H. Kum, S.-H. Bae, V. Bulovic, K.K. Yu, K. Chung, Y.J. Hong, A. Ougazzaden, J. Kim, Vertical full-colour micro-LEDs via 2D materials-based layer transfer, Nature 614 (2023) 81–87, https://doi.org/10.1038/s41586-022-05612-1.
[13] W.-T. Huang, Y.-H. Lin, P.-Y. Tu, L.T. Ngo, W.-C. Chen, K.-L. Liang, Y.-H. Fang, C. Su, R.-S. Liu, Enhancing color conversion of perovskite quantum dot-based micro-light-emitting diodes via electrochemical etching and flow chemistry system, Chem. Eng. J. 512 (2025) 162428, https://doi.org/10.1016/j.cej.2025.162428.
[14] J.-K. Kim, B.-S. Kim, J.-H. Jang, H.-S. Choi, B.-G. Ahn, M.-Y. Han, C.-J. Sung, J.-H. Baek, S.-J. Bae, W.-S. Shin, H.-W. Lee, S.-Y. Yoon, The latest milestone in WOLED technology for OLED TV and IT displays: enhancing efficiency, color gamut, and longevity, J. Soc. Inf. Disp. (2025) 1–8, https://doi.org/10.1002/jsid.2066.
[15] J. Huang, L. Yang, J. Feng, Z. Xu, L. Kan, H. Song, L. Huang, M. Huang, Z. Li, A. Pan, Solvent-mediated synthesis of small-sized perovskite quantum dots for a color-enhanced micro-LED display, ACS Nano 19 (2025) 22190–22206, https://doi.org/10.1021/acsnano.5c03449.
[16] C.A. Annis, Comparative cost, benefit, and adoption analysis of color filter on encapsulation (COE) to circular polarizers (C-POL) in anti-reflective film applications for OLED displays, SID Symp. Dig. Tech. Pap. 56 (2025) 217–220, https://doi.org/10.1002/sdtp.18128.
[17] C.X. Xu, S. Shu, J.N. Lu, G.C. Yuan, Q. Yao, L. Wang, Z.Q. Xu, Z.Y. Sun, Foldable AMOLED display utilizing novel COE structure, SID Symp. Dig. Tech. Pap. 49 (2018) 310–313, https://doi.org/10.1002/sdtp.12548.
[18] J. Jo, S.-R. Joung, S.M. Baik, C. Lee, H.-J. Kim, B.-C. Kwak, J.I. Lee, J.-Y. Yang, S. Yoon, High-luminance, large-size 4K OLED microdisplays for VR/MR applications, J. Soc. Inf. Disp. 32 (2024) 371–378, https://doi.org/10.1002/jsid.1301.
[19] S. Sim, J. Ryu, D.H. Ahn, H. Cho, C.-M. Kang, J.-W. Shin, C.W. Joo, G.H. Kim, C.-W. Byun, N.S. Cho, H.M. Youn, Y.J. An, J.S. Kim, H. Jung, H. Lee, Color gamut change by optical crosstalk in high-resolution organic light-emitting diode microdisplays, Opt. Express 30 (2022) 24155–24165, https://doi.org/10.1364/OE.463095.
[20] Y. Lin, Y. Yin, F. Zhang, Z. Liu, Cross talk in full-color micro-LED displays, Opt. Lett. 50 (2025) 2530–2533, https://doi.org/10.1364/OL.555035.
[21] Y.W. Kim, J.H. Kwon, H.-R. Choi, J.G. Choi, O.K. Kwon, K.H. Kim, E.H. Cho, T.-Y. Lee, E.-S. Cho, S.J. Kwon, Y. Jeon, Wearable quantum dots organic light-emitting diodes patch for high-power near infra-red photomedicine with real-time wavelength control, Chem. Eng. J. 499 (2024) 156121, https://doi.org/10.1016/j.cej.2024.156121.
[22] J.H. Sim, H. Chae, S.-B. Kim, S.B. Shin, H.K. Hong, H. Cho, Y.H. Jung, D. Lee, M. Kim, S. Hahn, S.J. Woo, S. Yoo, Wireless organic light-emitting diode contact lenses for on-eye wearable light sources and their application to personalized health monitoring, ACS Nano 19 (2025) 17478–17489, https://doi.org/10.1021/acsnano.4c18563.
[23] C. Kim, K. Lee, J. Kim, D. Yang, H. Lee, G. Moon, Y. Kim, D. Cho, K.S. Bae, G. Kim, Y. Kim, C. Lee, Multi-point sensing organic light-emitting diode display-based mobile cardiovascular monitor, Nat. Commun. 16 (2025) 1666, https://doi.org/10.1038/s41467-025-56915-6.
[24] D. Choi, S. Lee, H. Lee, R. Sharma, J. Kim, W. Lee, J. Park, S. Yoo, Vertically stacked all-organic ring-shaped pulse oximetry sensor with ultra-low power consumption and low-luminance operation, NPJ Flexible Electron. 9 (2025) 26, https://doi.org/10.1038/s41528-025-00395-7.

[25] C. Kant, M. Seetharaman, S. Mahmood, M. Katiyar, Single-step inkjet-printed dielectric template for large area flexible signage and low-information displays, ACS Nano 17 (2023) 22313–22325, https://doi.org/10.1021/acsnano.3c03903.
[26] K.-Y. Chen, A. Biswas, S. Cai, J. Huang, J. Andrews, Inkjet printed potentiometric sensors for nitrate detection directly in soil enabled by a hydrophilic passivation layer, Adv. Mater. Technol. 9 (2024) 2301140, https://doi.org/10.1002/admt.202301140.
[27] J. Park, J.-H. Lee, J. Lee, H. Cho, Effect of a P-doped hole transport and charge generation layer on single and two-tandem blue top-emitting organic light-emitting diodes, J. Inf. Disp. 22 (2021) 107, https://doi.org/10.1080/15980316.2020.1863273.
[28] S. Choi, C.-M. Kang, C.-W. Byun, H. Cho, B.-H. Kwon, J.-H. Han, J.-H. Yang, J.-W. Shin, C.-S. Hwang, N.S. Cho, K.M. Lee, H.-O. Kim, E. Kim, S. Yoo, H. Lee, Thin-film transistor-driven vertically stacked full color organic light-emitting diodes for high resolution active-matrix displays, Nat. Commun. 11 (2020) 2732, https://doi.org/10.1038/s41467-020-16551-8.
[29] S. Jang, J. Moon, H. Cho, C.W. Joo, J. Lee, J.-W. Shin, S.K. Park, N.S. Cho, S. Y. Yang, B.-H. Kwon, Spontaneously formed organic wrinkle structure for top-emitting organic light emitting diodes, J. Ind. Eng. Chem. 80 (2019) 490–496, https://doi.org/10.1016/j.jiec.2019.08.033.
[30] D. Kim, C.W. Joo, J.-W. Shin, H. Cho, C.-M. Kang, S. Choi, D.H. Ahn, C.W. Byun, N. S. Cho, K. Kim, I.-B. Baek, H. Suh, S.W. Woo, J. Lee, B.-H. Kwon, Fabrication of sub-micron organic/inorganic hybrid thin-film encapsulation on ultra-high-resolution microdisplays using inkjet printing process, SID Symp. Dig. Tech. Pap. 55 (2024) 1348–1351, https://doi.org/10.1002/sdtp.17796.
[31] D.V. Kuksenkov, B.-H. Kwon, C. Zhang, K.R. Allen, J.-W. Shin, C.-M. Kang, J. Kim, Quantum-dot-based color filter array for reflective displays, SID Symp. Dig. Tech. Pap. 56 (2025) 1348–1350, https://doi.org/10.1002/sdtp.18436.
[32] G. Shi, K. Baek, S.H. Ahn, J. Bae, J. Kim, L.S. Park, Synthesis of new binder polymers for photolithographic patterning of black pixel defining layers of organic light emitting diode, Mater. Sci. Appl. 10 (2019) 687–696, https://doi.org/10.4236/msa.2019.1011049.
[33] M. Lee, J. Bae, S. Ahn, B. Lee, High resolution black color patterns fabricated by photolithography with a novel high adhesion polymer for pixel defining layer of OLED, SID Symp. Dig. Tech. Pap. 49 (2018) 1782–1784, https://doi.org/10.1002/sdtp.12395.
[34] Y. Shin, H. Suh, B.-H. Kwon, J. Park, H. Cho, C.W. Joo, S. Choi, J.-W. Shin, C.-M. Kang, D.H. Ahn, W.J. Lee, Y.-H. Kim, J. Jang, B.-S. Bae, Environmentally stable luminescent perovskite nanocrystals passivated and encapsulated by siloxane hybrids enabling reliable color-converted organic light-emitting diodes, Chem. Eng. J. 474 (2023) 145889, https://doi.org/10.1016/j.cej.2023.145889.
[35] S.Y. Lee, C. Sakong, B.-K. Ju, K.H. Cho, Enhancing the reliability of InP-based QD color conversion layer through a uniform organic encapsulation layer via inkjet printing, Org. Electron. 135 (2024) 107136, https://doi.org/10.1016/j.orgel.2024.107136.
[36] I.J.-L. Plante, A. Barron, J. Yamanaga, M.J. Bautista, J. Tillman, X. Wang, H. Antoniadis, J. Yurek, Quantum dot color conversion for displays, SID Symp. Dig. Tech. Pap. 54 (2023) 792–794, https://doi.org/10.1002/sdtp.16681.
[37] Q. Li, F. Ma, X. Peng, T. Gao, B. Xu, L. Huang, J. Bai, Q. Li, W. Zhao, Dynamic color-tunable luminescence in lead-free perovskites by asymmetric energy transfer and excitation-dependent dual self-trapped excitons emission, Chem. Eng. J. 521 (2025) 166819, https://doi.org/10.1016/j.cej.2025.166819.
[38] S. Kim, S. Kang, S. Baek, J. Song, N.-E. Mun, H. Kwon, H.-G. Kwon, Y.-J. Pu, T.-W. Lee, S. Yoo, J.-M. Oh, J. Park, S.-W. Kim, Highly thin film with aerosol-deposited perovskite quantum dot/metal oxide composite for perfect color conversion and luminance enhancement, Chem. Eng. J. 441 (2022) 135991, https://doi.org/10.1016/j.cej.2022.135991.
[39] F. Qin, C. Liu, W. Wu, W. Peng, S. Huo, J. Ye, S. Gu, Inkjet printed quantum dots color conversion layers for full-color micro-LED displays, Electron. Mater. Lett. 19 (2023) 19–28, https://doi.org/10.1007/s13391-022-00373-5.
[40] J.M. Richardot, S. Kim, S. Jung, Evaluating inkjet printability of viscoelastic ink through Deborah number analysis, Phys. Fluids 37 (2025) 023135, https://doi.org/10.1063/5.0253639.
[41] S. Kim, R. Wenger, O. Bürgy, G. Balestra, U. Jeong, S. Jung, Predicting inkjet jetting behavior for viscoelastic inks using machine learning, Flex. Print. Electron. 8 (2023) 035007, https://doi.org/10.1088/2058-8585/acee94.
[42] H. Yoshida, S. Nakatani, Y. Usui, D. Wakabayashi, F. Ohtsuka, High-precision and high-stability inkjet printing technology for QD color converter-type micro-LED display, SID Symp. Dig. Tech. Pap. 31 (2023) 316–327, https://doi.org/10.1002/sdtp.17733.
[43] H. Yoshida, S. Nakatani, T. Inoue, Y. Usui, F. Ohtsuka, Mura-free G8.5 220 ppi inkjet printing technology for OLED and QLED display panels, J. Soc. Inf. Disp. 32 (2024) 255–266, https://doi.org/10.1002/jsid.1289.